

Mixed convection from an arbitrarily inclined semi-infinite flat plate—I. The influence of the inclination angle

G. WICKERN†

Institut für Thermo- und Fluidodynamik, Ruhr-Universität, Bochum, F.R.G.

(Received 14 September 1989)

Abstract—The laminar boundary layer flow over an arbitrarily inclined semi-infinite flat plate, either heated or cooled, is studied to determine the influence of the buoyancy forces on the basic forced convection flow. The complete range of inclination angles including the special cases of the horizontal and the vertical plate is covered by taking into account both components of the gravity vector, normal and parallel to the surface. The systematical variation of free parameters is continued by studying different thermal boundary conditions and by variation of the Prandtl number (discussed in Part II). One remarkable result of this study is the finding, that for opposing buoyancy forces singular as well as regular behaviour can occur.

1. INTRODUCTION

MIXED convection from horizontal and vertical plates has already been studied extensively by numerous authors [1–7], but only a few contributions have been made for the plate with arbitrary inclination angle. Although it can be stated in general that the buoyancy forces at an arbitrarily inclined plate have the same effect as those in an analogous boundary layer at the vertical plate, if only the component of the gravity vector parallel to the plate is taken into account, this is no longer true for horizontal or nearly horizontal surfaces. In the study of Jones [8] on free convection from flat plates slightly inclined to the horizontal it is demonstrated that there are two different mechanisms of buoyancy force influence on the boundary layer flow. These two mechanisms are associated with the two components of the gravity vector, parallel and normal to the surface. An example, where only the parallel component exists, is the free convection from the vertical plate, which was analysed first by Pohlhausen [9]. Since the flow in this case is driven by the buoyancy forces directly, this kind of free convection is denoted here 'direct free convection'. For the horizontal flat plate only the component of the gravity vector normal to the surface exists. Nevertheless, a boundary layer type flow parallel to the surface can be generated by heating the upper side of the plate, as was demonstrated by Stewartson [10]. An internal favourable pressure gradient parallel to the plate is induced by the buoyancy forces working normal to the plate, thus driving the flow indirectly. Therefore, this effect is denoted here 'indirect free convection'. Thus three physical mechanisms driving the flow have to be taken into account: the forced

convection due to the oncoming uniform main stream, the indirect free convection and the direct free convection. Therefore, in a mixed convection flow at an inclined surface two buoyancy parameters as ratios of two out of the three convection effects are needed to describe the behaviour of the boundary layer flow.

Mucoglu and Chen [11] demonstrated by a few examples for fixed Reynolds numbers that the indirect free convection is of importance only for plates with small inclination angles to the horizontal, but they did not identify both of the two independent buoyancy parameters. Thus a general solution for the inclined plate problem has not been given yet.

For opposing buoyancy forces flow separation is encountered. A Goldstein-type singularity was found by Merkin [4] for the mixed convection from the vertical plate held at a constant temperature. This result was confirmed by Hunt and Wilks [2], who in addition provided the solution for uniform surface heat flux. For mixed convection from the horizontal plate a similar type of singularity is expected. In the vicinity of the separation point numerical problems have been reported by several authors [5–7, 11, 12]. In contrast to this Jones [8] found a regular behaviour at the separation point for the problem of mixed indirect and direct free convection. Therefore, the determination of location and type of separation point was the most important question in the cases with opposing buoyancy forces.

2. BOUNDARY LAYER EQUATIONS

The configuration considered is sketched in Fig. 1. The boundary layer equations read (in dimensional form assuming laminar flow and that variable fluid properties can be taken into account by the Boussinesq approximation)

† Present address: Mercedes-Benz AG, 7032 Sindelfingen, Postfach 226, F.R.G.

NOMENCLATURE

c_f	friction coefficient, equation (17)	β	coefficient of thermal expansion
c_p	specific heat capacity	η	dynamic viscosity
e	exponent of temperature distribution, equation (7)	η_s	scaled y -coordinate for velocity boundary layer, equation (7)
f	scaled streamfunction, equation (7)	ϑ	reduced dimensionless temperature, equation (7)
g^*	gravitational acceleration	θ	dimensionless temperature
Gr	Grashof number, equation (5)	λ	thermal conductivity
$\hat{G}r$	modified Grashof number for $\dot{q}_w = \text{const.}$, equation (14)	ν	kinematic viscosity
L^*	reference length	ρ	density
N	y -coordinate scaled with $\sqrt{(Re)}$, equation (5)	τ_w	wall shear stress.
Nu	Nusselt number, equation (18)		
p	pressure		
Pe	Peclet number, $Re Pr$		
Pr	Prandtl number, equation (5)		
\dot{q}_w	wall heat flux		
Re	Reynolds number, equation (5)		
T	temperature		
u, \bar{v}	velocity components		
U_B	reference velocity		
U_∞	free-stream velocity		
x, y	coordinate system.		

Greek symbols			
α	inclination angle		

Subscripts			
s	scaled for the velocity boundary layer		
S	separation		
w	wall value		
x	local quantity		
∞	free-stream value.		

Superscripts			
*	dimensional quantity		
'	derivative with respect to η_s		
$\hat{\quad}$	modified for $\dot{q}_w = \text{const.}$		
$\bar{\quad}$	scaled quantity.		

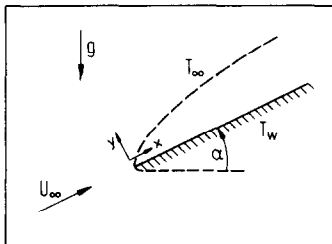


FIG. 1. The coordinate system for mixed convection from an arbitrarily inclined flat plate.

$$\frac{\partial u}{\partial x} + \frac{\partial \bar{v}}{\partial N} = 0 \quad (1)$$

$$u \frac{\partial u}{\partial x} + \bar{v} \frac{\partial u}{\partial N} = \frac{\partial^2 u}{\partial N^2} + \frac{Gr}{Re^2} \sin \alpha \theta - \frac{\partial p}{\partial x} \quad (2)$$

$$\frac{\partial p}{\partial N} = \frac{Gr}{Re^{5/2}} \cos \alpha \theta \quad (3)$$

$$u \frac{\partial \theta}{\partial x} + \bar{v} \frac{\partial \theta}{\partial N} = \frac{1}{Pr} \frac{\partial^2 \theta}{\partial N^2} \quad (4)$$

where

$$x = \frac{x^*}{L^*}, \quad N = \frac{y^*}{L^*} \sqrt{(Re)}, \quad p = \frac{p^* - p_{\text{stat } \infty}^*}{\rho_\infty^* U_\infty^{*2}}$$

$$u = \frac{u^*}{U_B^*}, \quad \bar{v} = \frac{v^*}{U_B^*} \sqrt{(Re)}, \quad \theta = \frac{T_w^* - T_\infty^*}{(T_w^* - T_\infty^*)}$$

$$Re = \frac{\rho_\infty^* U_B^* L^*}{\eta^*}, \quad Pr = \frac{c_{p\infty}^* \eta_\infty^*}{\lambda_\infty^*},$$

$$Gr = \frac{\beta^* \Delta T^* g^* L^{*3} \rho_\infty^{*2}}{\eta_\infty^{*2}} \quad (5)$$

(with $U_B^* = U^*$).

The pressure p is the deviation from the static pressure in the ambient, the so-called modified pressure. In contrast to Prandtl's classical boundary layer theory the pressure in the boundary layer is no longer determined by the pressure field outside. Nevertheless this is strictly in line with the boundary layer concept as an asymptotic theory for infinite Reynolds numbers.

The influence of direct free convection is represented by the buoyancy term in the x -momentum equation (2). The indirect free convection can be identified with the buoyancy term in the y -momentum equation (3). Thus the two dimensionless combinations in the buoyancy terms characterize the strength of the two buoyancy effects

$$\frac{Gr}{Re^2} \sin \alpha \cong \frac{\text{direct free convection}}{\text{forced convection}}$$

$$\frac{Gr}{Re^{5/2}} \cos \alpha \cong \frac{\text{indirect free convection}}{\text{forced convection}}$$

The governing equations (1)–(4) are subject to the following boundary conditions:

$$\begin{aligned}
 u(x, 0) &= 0, & \theta(x, 0) &= 1 & (T_w = \text{const.}) \\
 \bar{v}(x, 0) &= 0, & \frac{\partial \theta}{\partial N}(x, 0) &= \text{const.} & (\dot{q}_w = \text{const.}) \\
 u(x, \infty) &= 1, & \theta(x, \infty) &= 0 \\
 p(x, \infty) &= 0. & & & (6)
 \end{aligned}$$

To simplify the mathematical analysis the basic equations are rewritten in terms of the streamfunction ψ , thus satisfying the continuity equation (1) implicitly. The following similarity transformation is introduced in order to reduce the problem at the leading edge ($x = 0$) to the well-known Blasius solution and to keep x -derivatives finite in this region :

$$\begin{aligned}
 \eta_s &= x^{-1/2} N \\
 x_s &= x^{1/2+e} \\
 f &= x^{-1/2} \psi \\
 \vartheta &= x^{-e} \theta
 \end{aligned} \tag{7}$$

($e = 0$ for $T_w = \text{const.}$, $e = -\frac{1}{2}$ for $\dot{q}_w = \text{const.}$).

The transformed set of equations then is

$$\begin{aligned}
 f''' + \frac{1}{2} f f'' &= -x_s^{(2+2e)/(1+2e)} \frac{Gr}{Re^2} \sin \alpha \vartheta \\
 &\quad - \frac{1}{2} \eta_s x_s \frac{Gr}{Re^{5/2}} \cos \alpha \vartheta \\
 &\quad + x_s (\frac{1}{2} + e) \left(\frac{\partial p}{\partial x_s} + f' \frac{\partial f'}{\partial x_s} - \frac{\partial f}{\partial x_s} f'' \right) \tag{8}
 \end{aligned}$$

$$p' = x_s \frac{Gr}{Re^{5/2}} \cos \alpha \vartheta \tag{9}$$

$$\begin{aligned}
 \vartheta'' + \frac{1}{2} Pr f \vartheta' - e Pr f' \vartheta \\
 = Pr x_s (\frac{1}{2} + e) \left(f' \frac{\partial \vartheta}{\partial x_s} - \frac{\partial f}{\partial x_s} \vartheta' \right) \tag{10}
 \end{aligned}$$

(primes denote partial derivatives with respect to η_s , $e = 0$ for $T_w = \text{const.}$, $e = \frac{1}{2}$ for $\dot{q}_w = \text{const.}$). The transformed boundary conditions are

$$\left. \begin{aligned}
 f(x_s, 0) &= 0, & \vartheta(x_s, 0) &= 1, & T_w &= \text{const.} \\
 f'(x_s, 0) &= 0, & \vartheta(0, 0) &= 1 \\
 f'(x_s, \infty) &= 1, & \vartheta'(x_s, 0) &= \vartheta'(0, 0) \\
 p(x_s, \infty) &= 0, & \vartheta(x_s, \infty) &= 0.
 \end{aligned} \right\} \dot{q}_w = \text{const.} \tag{11}$$

The problem described by the above set of equations (8)–(11) still has four free parameters. Since the two buoyancy parameters are associated with the length scale L^* , which for a semi-infinite flat plate is purely formal, the number of free parameters can be reduced by one by introducing local quantities for the buoyancy parameters

$$\frac{Gr_x}{Re_x^2} \sin \alpha = x_s^{1+e} \frac{Gr}{Re^2} \sin \alpha \tag{12}$$

$$\frac{Gr_x}{Re_x^{5/2}} \cos \alpha = x_s^{1/2+e} \frac{Gr}{Re^{5/2}} \cos \alpha. \tag{13}$$

The wall values of the solution are now only functions of the two local buoyancy parameters, the Prandtl number and the temperature exponent e .

For the constant surface heat flux case this representation is still inadequate, since there is no well-defined temperature difference to form a suitable Grashof number. Thus a modified Grashof number is introduced especially for the constant heat flux case

$$\hat{Gr}_x \equiv \frac{\beta^* \dot{q}_w^* g^* x^{*4} \rho_x^{*2}}{\lambda_x^* \eta_x^{*2}}. \tag{14}$$

Adequate buoyancy parameters for the constant surface heat flux case according to this definition are

$$\frac{\hat{Gr}_x}{Re_x^{5/2}} \sin \alpha = x_s^{1+e} \frac{Gr}{Re^2} \sin \alpha (-\vartheta'(0, 0)) \tag{15}$$

$$\frac{\hat{Gr}_x}{Re_x^3} \cos \alpha = x_s^{1/2+e} \frac{Gr}{Re^{5/2}} \cos \alpha (-\vartheta'(0, 0)) \tag{16}$$

(with $e = \frac{1}{2}$ for $\dot{q}_w = \text{const.}$).

By these equations the buoyancy parameters that have to be fixed for the numerical calculations can be related to known quantities for the constant heat flux case.

The numerical results are presented as well in terms of dimensionless quantities. Wall shear stress is given in terms of the local friction coefficient c_{fx} . Heat transfer results are described by the local Nusselt number

$$c_{fx} = \frac{\tau_w^*}{\rho_x^* U_B^{*2}} = Re_x^{-1/2} f''(x_s, 0) \tag{17}$$

$$Nu_x = \frac{\dot{q}_w^* x^*}{\lambda_\infty^* (T_w^* - T_\infty^*)} = -Re_x^{1/2} (\vartheta'(x_s, 0) / \vartheta(x_s, 0)). \tag{18}$$

The reference velocity U_B^* usually is U_∞^* . For the case without main stream velocity (Fig. 4) a reference velocity based on a characteristic buoyancy quantity is introduced.

3. NUMERICAL RESULTS FOR $Pr = 0.72$

The governing set of equations (8)–(11) was solved numerically for $Pr = 0.72$ incorporating Keller's box scheme. A grid of typically 130 points in the y -direction was used. The complete set of equations, which was transformed into a system of six first-order differential equations, was solved simultaneously. The results are accurate to at least three significant digits. For details of the numerical solution see ref. [14].

Prior to analysing the general solution those cases with only two of the three physical mechanisms present will be considered. For mixed convection from a vertical flat plate only forced convection and direct free convection have to be taken into account. In Figs. 2(a)–(d) skin friction and heat transfer results for the vertical plate are plotted vs the local direct free

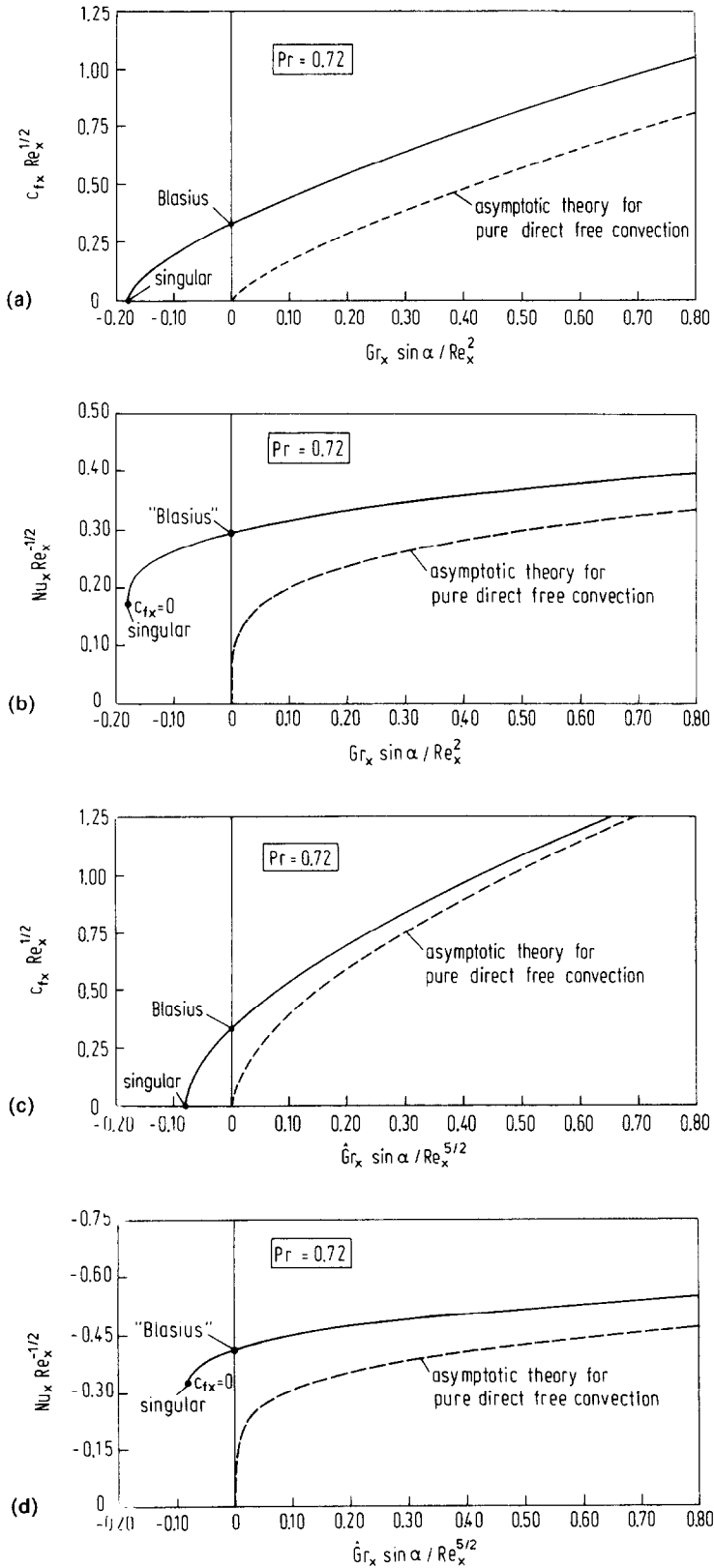


FIG. 2. Friction coefficient and Nusselt number for mixed convection from a vertical flat plate: (a), (b) constant wall temperature; (c), (d) constant surface heat flux.

convection buoyancy parameters. For aiding free convection both wall shear stress and heat transfer increase monotonically, whereas for opposing buoyancy forces both quantities decrease until separation occurs. The separation points are $Gr_x/Re_x^2 \sin \alpha|_S = -0.1806$ for constant wall temperature and $\hat{G}r_x/Re_x^{5/2} \sin \alpha|_S = -0.07918$ for constant surface heat flux. Both cases exhibit square-root singularity behaviour in the vicinity of the separation point. This singularity at separation has been investigated by Merkin [4] and by Hunt and Wilks [2]. They found it to be very similar to the well-known Goldstein singularity for separation due to an external pressure gradient.

Mixed convection from the horizontal plate is shown in Figs. 3(a)–(d). Here only forced and indirect free convection are present. Nevertheless the results are roughly similar to those for the vertical plate. The aiding case has been investigated by various authors [1, 5–7] and the results are no longer a point of discussion. But this is not true for the opposing case. For this case numerical results were supplied by Schneider and Wasel [7] and by Raju *et al.* [5]. Both studies claimed a singular behaviour at a point with finite positive wall shear stress. The numerical results of the present study cannot support these findings, although it must be stated, that for all cases with opposing indirect free convection the numerical solution is extremely difficult. A detailed discussion of the numerical problems, which cannot be regarded as fully understood, is given in ref. [14]. Nevertheless the new numerical data are believed to be the most reliable results available for the problem.

The solution near separation again is of the square-root-singularity type with the origin of the singularity fixed at the point of zero wall shear stress. Up to now, the basis for this statement is more or less empirical leaving the answer to a theoretical investigation following the lines of the analysis by Goldstein [13] and Stewartson [15]. The separation points predicted for the horizontal flat plate are $Gr_x/Re_x^{5/2} \cos \alpha|_S = -0.08878$ for the constant wall temperature and $\hat{G}r_x/Re_x^3 \cos \alpha|_S = -0.03120$ for the constant surface heat flux case. As for the vertical plate the heat transfer remains finite at separation, although a strong gradient for the heat transfer rate is found near the singularity.

A third case with only two of the three mechanisms present is the *free* convection from a slightly inclined horizontal plate. The basic indirect free convection is disturbed by the direct free convection buoyancy forces, either in an aiding or in an opposing manner. For this flow the initial solution at $x = 0$ is not the Blasius profile, so that equation (7) is no longer adequate. In addition different buoyancy parameters, $(Gr_x \cos \alpha)^{1/5} \cos \alpha$ for $T_w = \text{const.}$ and $(\hat{G}r \cos \alpha)^{1/6} \times \tan \alpha$ for $\dot{q}_w = \text{const.}$, have to be introduced. The resulting equations are not given here, since they are given in Jones [8], who investigated this problem for the first time (only $T_w = \text{const.}$), and in ref. [14] (both T_w and $\dot{q}_w = \text{const.}$).

The most important feature of the solution by Jones was the complete regularity at the point of vanishing skin friction. Although a strong growth of boundary layer thickness was observed in the separated flow region, the growth rate remained finite for all x . This increase in boundary layer thickness is part of the mechanism enabling the solution to stay regular at separation. The effect of indirect free convection, which is responsible for the original forward flow, is proportional to the boundary layer thickness. Thus the boundary layer growth enhances the forward flow again, as soon as a backward flow region begins to develop. Thus a balance between aiding and opposing buoyancy forces is kept even beyond the separation point. Mathematically this balance manifests itself in the non-trivial y -momentum equation (3).

By means of the nowadays largely extended computational facilities it was possible to extend Jones' solution further downstream. In addition the analysis was extended to include the constant surface heat flux boundary condition. The results are sketched in Figs. 4(a)–(d) (in c_{fx} now $U_B^* = (\beta^* \Delta T^* \cos \alpha g^* L^{*-1/2} \nu^{1/2})^{2/5}$). It should be pointed out that for opposing direct free convection the negative skin friction in the backward flow region does not grow monotonically, but takes a maximum and then decreases again tending to zero asymptotically. The structure of the separated flow far beyond the point of zero skin friction, which can be analysed by the method of matched asymptotic expansions, will be discussed in an additional paper [16].

In the constant heat flux results a strange oscillation of the friction coefficient occurs in the separated region. Up to seven zeroes could be resolved by the numerical computations. Probably there is no physical counterpart for this solution behaviour; nevertheless the solution obviously is correct from a purely mathematical point of view and it is of some interest due to its curiosity. The velocity profiles of this solution (not given here, see ref. [14]) have as many zeroes as the skin friction distribution upstream of the x location under consideration.

The location of the separation point is $(Gr_x \times \cos \alpha)^{1/5} \tan \alpha|_S = -2.224$ for $T_w = \text{const.}$ and $(\hat{G}r_x \cos \alpha)^{1/6} \tan \alpha|_S = -2.830$ for $\dot{q}_w = \text{const.}$, respectively.

The heat transfer results are similar for both thermal boundary conditions. In the aiding case the transfer rate is increasing monotonically, whereas in the opposing case it decreases and finally tends to zero. This is due to the strong boundary layer growth for the separated flow resulting in a vanishing temperature gradient at the wall.

A special diagram has been developed to present the complete solution in one picture, sketched in Fig. 5. Solutions already known from the literature are included with their range of validity. Skin friction and heat transfer results can be plotted as contour maps into the plane defined by the two local buoyancy parameters. For any given configuration $(\beta^*, \Delta T^*, g^*,$

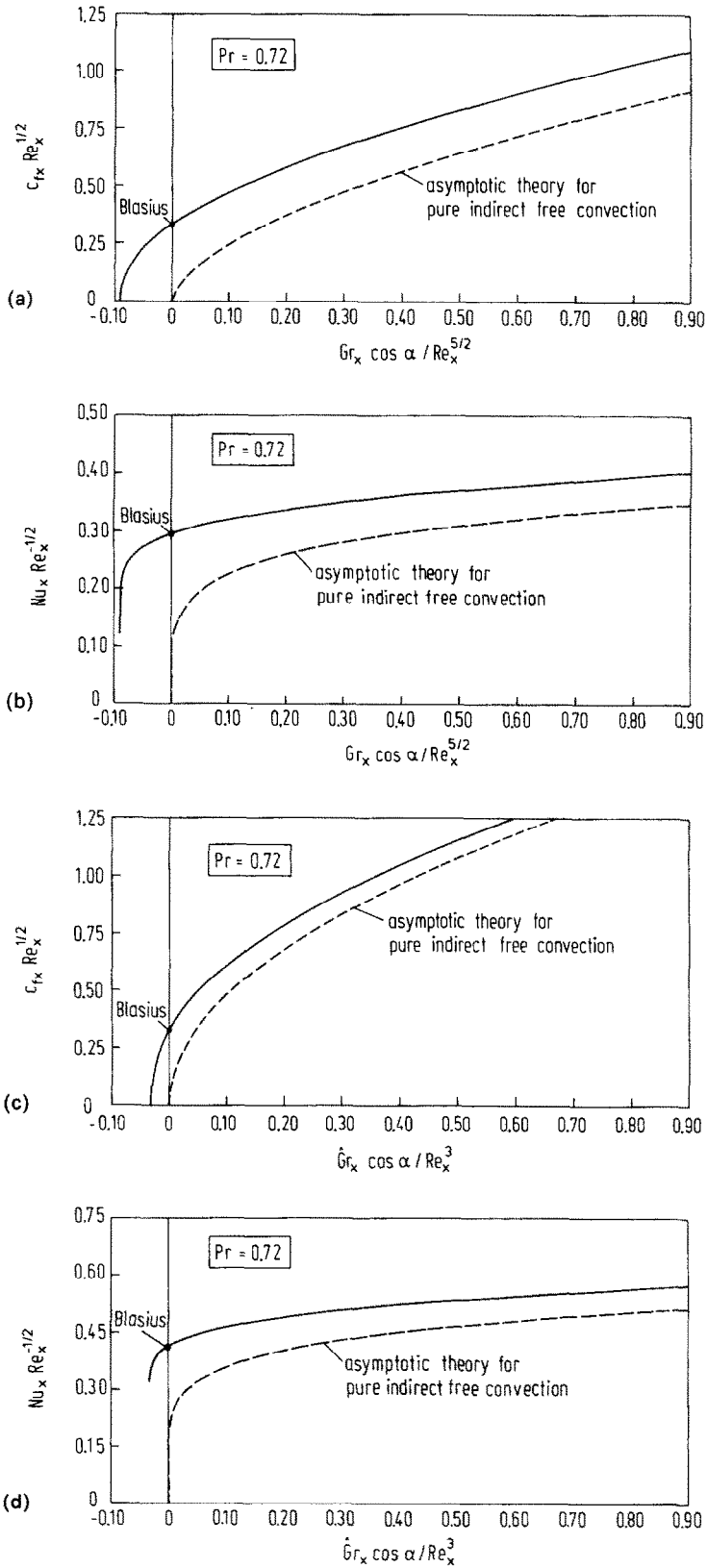


FIG. 3. Friction coefficient and Nusselt number for mixed convection from a horizontal flat plate: (a), (b) constant wall temperature; (c), (d) constant surface heat flux.

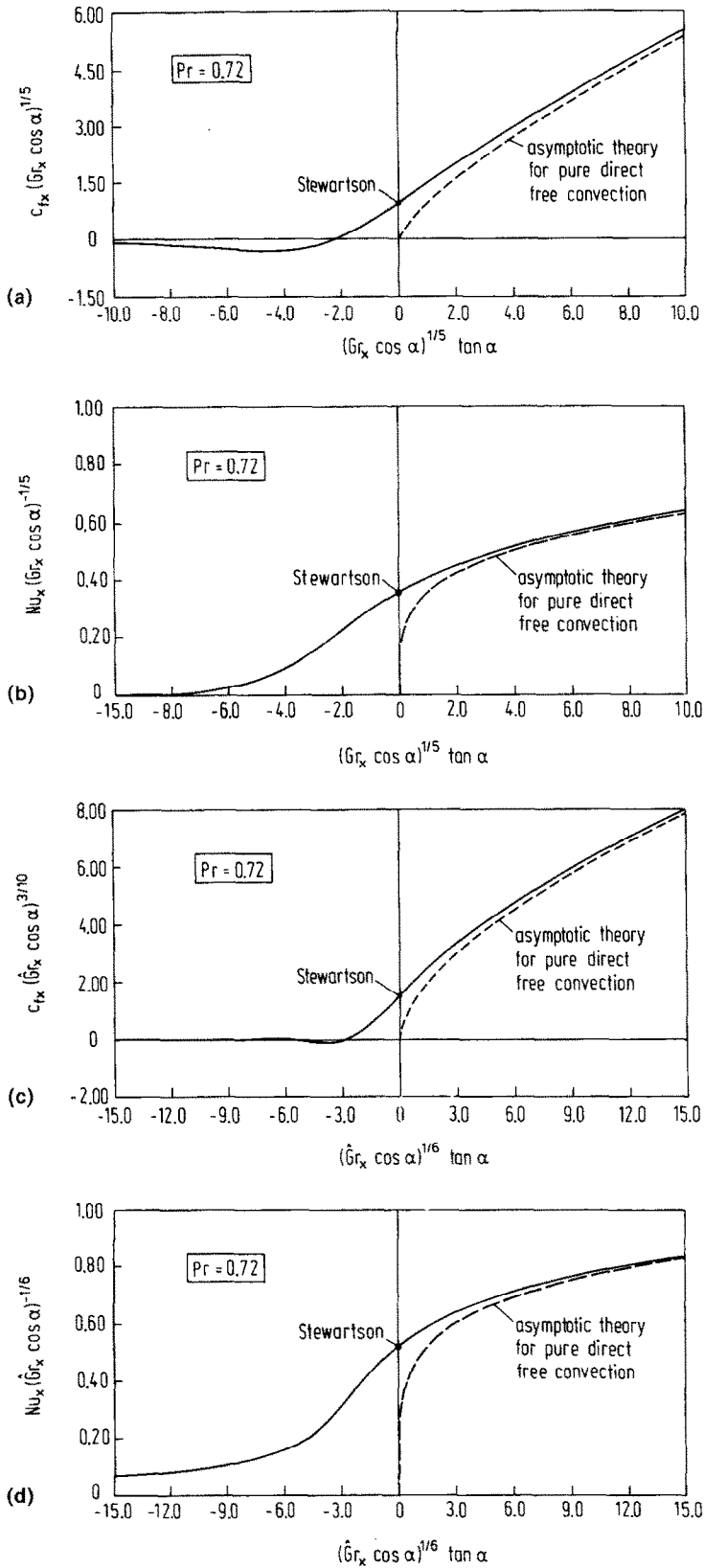


FIG. 4. Friction coefficient and Nusselt number for free convection from a flat plate slightly inclined to the horizontal: (a), (b) constant wall temperature; (c), (d) constant surface heat flux.

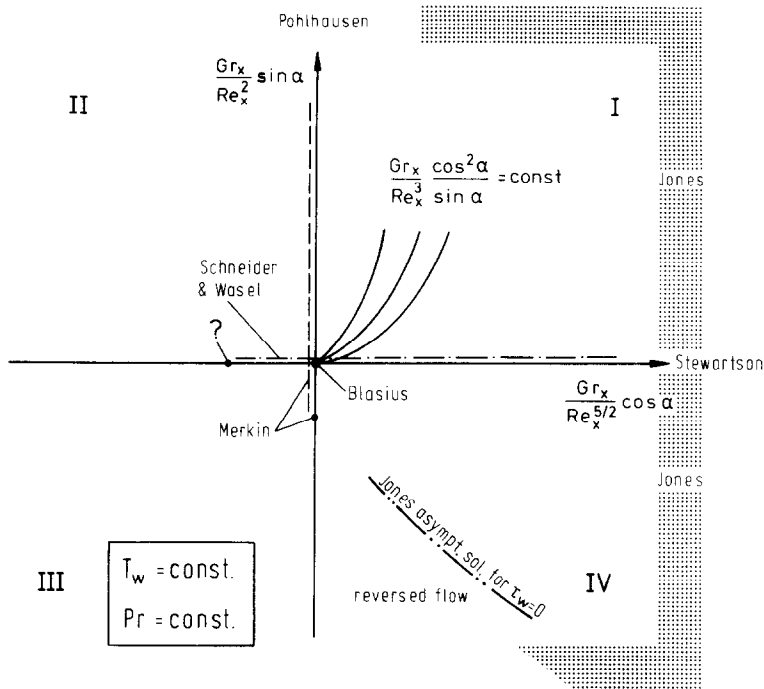


FIG. 5. Structure of a contour map for the complete solution for mixed convection from inclined plates with references to solutions known from the literature.

α^*, v^*, U_x^*) the solution for growing x is located on parabolas beginning in the mid-point of the diagram. The parabola for a certain configuration can be identified by a dimensionless x -independent parameter combining the original buoyancy parameters. For the constant wall temperature case this combination is

$$\frac{Gr \cos^2 \alpha}{Re^3 \sin \alpha} = \frac{\left(\frac{Gr_x}{Re_x^{5/2}} \cos \alpha \right)^2}{\frac{Gr_x}{Re_x^2} \sin \alpha}$$

for the constant surface heat flux case it is

$$\frac{\hat{G}r \cos^3 \alpha}{Re^4 \sin^2 \alpha} = \frac{\left(\frac{\hat{G}r_x}{Re_x^3} \cos \alpha \right)^3}{\left(\frac{\hat{G}r_x}{Re_x^{5/2}} \sin \alpha \right)^2}$$

Only two free parameters are left in the diagram, the thermal boundary condition and the Prandtl number. In Figs. 6(a) and (b) the results for the case $T_w = \text{const.}$ are shown together with a solution for vanishing mainstream velocity. This asymptotic solution can be extracted from Jones' study of free convection at the flat plate slightly inclined from the horizontal. From these pictures it can be concluded that the solution on the right-hand side of the diagram ($Gr_x / Re_x^{5/2} \cos \alpha > 0$) is similar to the one given by Jones (Fig. 5) with regular behaviour at separation. For $Gr_x / Re_x^{5/2} \cos \alpha \leq 0$ (left-hand side of the diagram) the solution is roughly similar to the singular solu-

tions of Figs. 3 and 4. Thus major parts of the diagram (left-hand side) cannot be filled by boundary layer theory calculations. The parabola marked in the upper left part is the limiting case of marginal separation. For a solution in the left neighbourhood of this line, a separation bubble would exist in the real flow. The numerical boundary layer solution is terminated by a singularity at the onset of backflow. The same mechanism that keeps the solutions regular in the right half of the diagram supports the singularity in the left half. In both cases the opposing buoyancy forces are enhanced by the boundary layer growth.

The results for $\hat{q}_w = \text{const.}$ in Figs. 7(a) and (b) are qualitatively similar to those for $T_w = \text{const.}$ The only major differences occur in the lower right part of the diagram where regular separation is found. These differences are principally the same as those for pure free convection in Figs. 5(a) and (c).

The singularity found by Merkin for mixed convection at the vertical plate is an important point in all these diagrams. This solution obviously marks the limit between singular and regular behaviour at separation. In the vicinity of this point the gradients observed in the contour plots are increasing strongly with decreasing distance to the singularity. The development of Merkin's singularity from the original regular behaviour can be analysed by an asymptotic approach, which will be discussed in a subsequent paper [16].

Since the results in the upper right parts of the contour maps (purely accelerated flows) have a rather simple structure, it was possible to represent these

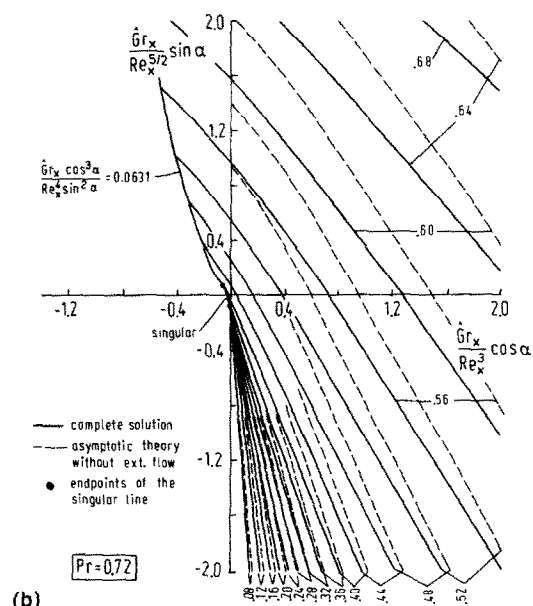
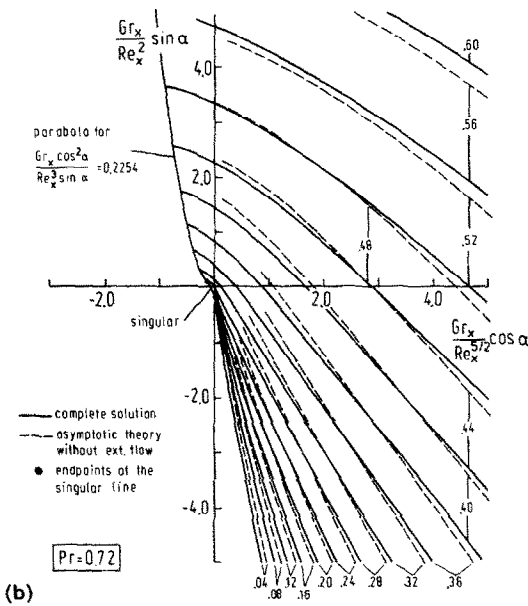
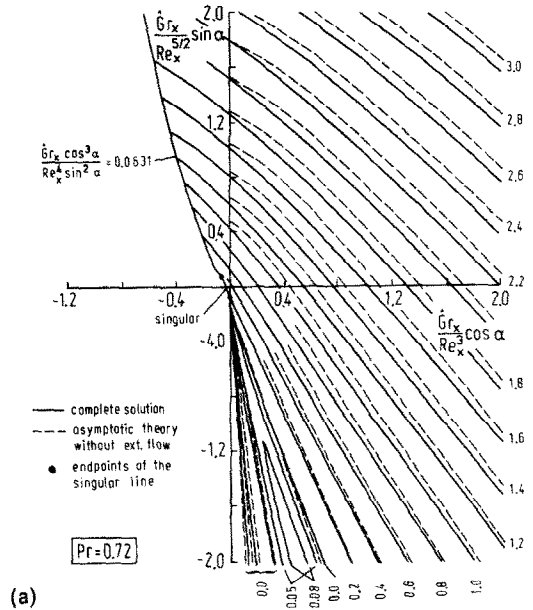
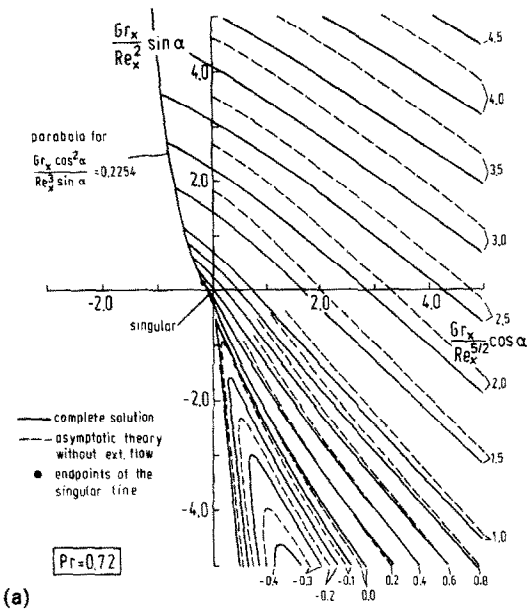


FIG. 6. Contour maps with results for mixed convection from inclined plates for the constant wall temperature case: (a) friction coefficient, lines of constant $c_{fx} Re_x^{1/2}$; (b) Nusselt number, lines of constant $-Nu_x Re_x^{-1/2}$.

FIG. 7. Contour maps with results for mixed convection from inclined plates for the constant surface heat flux case: (a) friction coefficient, lines of constant $c_{fx} Re_x^{1/2}$; (b) Nusselt number, lines of constant $-Nu_x Re_x^{-1/2}$.

results by correlation equations. Such simple equations make the numerical data easily accessible for practical use, reducing the huge amount of data to a few constants. The correlation equations and their derivation are described in the Appendix.

4. CONCLUSIONS

A systematic approach covering all cases of mixed convection from an inclined flat plate has been developed. The dependence of the local skin friction coefficient and Nusselt number on the inclination

angle, on the thermal boundary condition, and on the fluid properties has been reduced into an adequate set of dimensionless numbers and then been discussed qualitatively on the basis of plotted results of the numerical solution. For a qualitative survey of the solutions, a special contour map diagram has been developed showing friction coefficients or Nusselt numbers over a plane defined by the two local buoyancy parameters. Quantitative results are provided for the accelerated flow cases by means of simple correlations given in the Appendix covering the whole range of free parameters including the influence of the

Prandtl number, although the detailed analysis for low and high Prandtl numbers will be given in Part II. For the cases with opposing buoyancy forces the separation points have been determined and the behaviour in the vicinity of the point of zero skin friction has been analysed whether the separation is singular or regular. A more detailed discussion of the phenomena encountered during the analysis of regular and singular separated flows will be given in an additional paper.

Acknowledgements—The author would like to thank Prof. Dr K. Gersten and Prof. Dr H. Herwig for many valuable discussions. The project was supported by the Deutsche Forschungsgemeinschaft under contract Ge 147/19-1.

REFERENCES

1. T. S. Chen, E. M. Sparrow and A. Mucoglu, Mixed convection in boundary layer flow on a horizontal plate, *J. Fluid Mech.* **99**, 66–71 (1977).
2. R. Hunt and G. Wilks, On the behavior of the laminar boundary layer equations of mixed convection near a point of zero skin friction, *J. Fluid Mech.* **101**, 377–391 (1980).
3. L. G. Leal, Combined forced and free convection heat transfer from a horizontal flat plate, *ZAMP* **24**, 20–42 (1973).
4. J. H. Merkin, The effect of buoyancy forces on the boundary-layer flow over a semi-infinite vertical flat plate in a uniform stream, *J. Fluid Mech.* **35**, 439–450 (1969).
5. M. S. Raju, X. Q. Lui and C. K. Law, A formulation of combined forced and free convection past horizontal and vertical surfaces, *Int. J. Heat Mass Transfer* **27**, 2215–2224 (1984).
6. N. Ramachandran, B. F. Armaly and T. S. Chen, Mixed convection over a horizontal plate, *J. Heat Transfer* **105**, 420–432 (1983).
7. W. Schneider and M. G. Wasel, Breakdown of the boundary layer approximation for mixed convection above a horizontal plate, *Int. J. Heat Mass Transfer* **28**, 2307–2313 (1985).
8. D. R. Jones, Free convection from a semi-infinite flat plate inclined at a small angle to the horizontal, *Q. J. Mech. Appl. Math.* **26**, 77–97 (1973).
9. E. Pohlhausen, Der Wärmeaustausch zwischen festen Körpern und Flüssigkeiten mit kleiner Reibung und kleiner Wärmeleitung, *ZAMM* **1**, 115–121 (1921).
10. K. Stewartson, On the free convection from a horizontal plate, *ZAMP* **9a**, 276–282 (1958).
11. A. Mucoglu and T. S. Chen, Mixed convection on inclined surfaces, *J. Heat Transfer* **101**, 422–426 (1979).
12. N. Ramachandran, B. F. Armaly and T. S. Chen, Measurements of laminar mixed convection flow adjacent to an inclined surface, *J. Heat Transfer* **109**, 146–150 (1987).
13. S. Goldstein, On laminar boundary-layer flow near a position of separation, *Q. J. Mech. Appl. Math.* **1**, 43–69 (1948).
14. G. Wickern, Untersuchung der laminaren gemischten Konvektion an einer beliebig geneigten ebenen Platte mit besondere Berücksichtigung der Strömungsablösung, *Fortschr.-Ber. VDI* **7**, Nr. 129 (1987).
15. K. Stewartson, On Goldstein's theory of laminar separation, *Q. J. Mech. Appl. Math.* **11**, 399–410 (1958).
16. G. Wickern, Asymptotic description of separation regions in a class of mixed convection flows. To appear.
17. S. W. Churchill and R. Usagi, A general expression for the correlation of rates of transfer and other phenomena, *A.I.Ch.E. J.* **18**, 1121–1128 (1972).

APPENDIX

Following a proposal by Churchill and Usagi [17] a simple correlation can be derived from the self-similar solutions of the basic flows of pure forced and pure free convection. Thus the huge amount of data produced during the numerical solution of the complete partial differential equations can be reduced to a form suitable for publication. The results of the correlation were tested versus the exact numerical solution and a maximum error of 5% was found.

There are two sets of correlation equations corresponding to the two different thermal boundary conditions $T_w = \text{const.}$ and $\dot{q}_w = \text{const.}$ investigated, whereas the dependence on the Prandtl number and on the two buoyancy parameters is taken into account by explicit occurrence of these quantities in the correlations.

$T_w = \text{const.}$:

$$c_{f_x} = Re_x^{-1/2} \left\{ \left[(f_{1c})^{1.2} + \left[f_{3c} \left(\frac{Gr_x}{Re_x^2} \sin \alpha \right)^{3.4} \right]^{1.2} \right]^{1.3/1.2} + \left[f_{2c} \left(\frac{Gr_x}{Re_x^{5/2}} \cos \alpha \right)^{3.5} \right]^{1.3} \right\}^{1/1.3}$$

$$Nu_x = Re_x^{1/2} \left\{ (f_{1N})^{3.2} + \left[f_{3N} \left(\frac{Gr_x}{Re_x^2} \sin \alpha \right)^{1.4} \right]^{3.2} + \left[f_{2N} \left(\frac{Gr_x}{Re_x^{5/2}} \cos \alpha \right)^{1.5} \right]^{3.2} \right\}^{1/3.2}$$

$\dot{q}_w = \text{const.}$:

$$\hat{c}_{f_x} = Re_x^{-1/2} \left\{ \left[(\hat{f}_{1c})^{1.8} + \left[\hat{f}_{3c} \left(\frac{\hat{Gr}_x}{Re_x^{5/2}} \sin \alpha \right)^{3.5} \right]^{1.8} \right]^{1.7/1.8} + \left[\hat{f}_{2c} \left(\frac{\hat{Gr}_x}{Re_x^3} \cos \alpha \right)^{1.2} \right]^{1.7} \right\}^{1/1.7}$$

$$\hat{Nu}_x = Re_x^{1/2} \left\{ (\hat{f}_{1N})^{3.4} + \left[\hat{f}_{3N} \left(\frac{\hat{Gr}_x}{Re_x^{5/2}} \sin \alpha \right)^{1.5} \right]^{3.4} + \left[\hat{f}_{2N} \left(\frac{\hat{Gr}_x}{Re_x^3} \cos \alpha \right)^{1.6} \right]^{3.4} \right\}^{1/3.4}$$

with the results from forced convection similarity solutions

$$f_{1c} = 0.3320$$

$$f_{1N} = [(0.5642Pr^{1/2})^{-4.6} + (0.3387Pr^{1/3})^{-4.6}]^{-1/4.6}$$

$$\hat{f}_{1c} = 0.3320$$

$$\hat{f}_{1N} = [(0.8862Pr^{1/2})^{-4.6} + (0.4636Pr^{1/3})^{-4.6}]^{-1/4.6}$$

and with results from indirect free convection similarity solutions

$$f_{2c} = [(1.231Pr^{-3/10})^{-3.2} + (0.9753Pr^{-2/5})^{-3.2}]^{-1/3.2}$$

$$f_{2N} = [(0.5755Pr^{2/5})^{-2.7} + (0.4562Pr^{1/5})^{-2.7}]^{-1/2.7}$$

$$\hat{f}_{2c} = [(1.525Pr^{-1/2})^{-12.5} + (1.300Pr^{-1/2})^{-12.5}]^{-1/12.5}$$

$$\hat{f}_{2N} = [(0.8309Pr^{1/3})^{-3.2} + (0.6231Pr^{1/6})^{-3.2}]^{-1/3.2}$$

and with results from direct free convection similarity solutions

$$f_{3c} = [(1.513)^{-1.9} + (1.166Pr^{-1/4})^{-1.9}]^{-1/1.9}$$

$$f_{3N} = [(0.6004Pr^{1/2})^{-2.3} + (0.5028Pr^{1/4})^{-2.3}]^{-1/2.3}$$

$$\hat{f}_{3c} = [(1.756Pr^{-3/10})^{-4.0} + (1.546Pr^{-2/5})^{-4.0}]^{-1/4.0}$$

$$\hat{f}_{3N} = [(0.7609Pr^{2/5})^{-2.8} + (0.6316Pr^{1/5})^{-2.8}]^{-1/2.8}$$

CONVECTION MIXTE SUR UNE PLAQUE PLANE SEMI-INFINIE—I. INFLUENCE DE L'ANGLE D'INCLINAISON

Résumé—La couche limite laminaire sur une plaque plane semi-infinie arbitrairement inclinée, chauffée et refroidie, est étudiée pour déterminer l'influence des forces de flottement sur l'écoulement forcé de base. Le domaine complet d'angle d'inclinaison incluant les cas particuliers de la plaque horizontale et verticale est considéré en prenant en compte à la fois les composantes du vecteur gravité, normale et parallèle à la surface. La variation systématique des paramètres libres est faite en étudiant différentes conditions aux limites thermiques et différents nombres de Prandtl (discussion en seconde partie). Un résultat remarquable de cette étude est que pour des forces de flottement en opposition il peut apparaître un comportement régulier aussi bien que singulier.

GEMISCHTE KONVEKTION AN EINER BELIEBIG GENEIGTEN HALBUNENDLICHEN PLATTE—I. DER EINFLUSS DES ANSTELLWINKELS

Zusammenfassung—Die laminare Grenzschichtströmung an einer beliebig geneigten halb-unendlichen ebenen Platte, die entweder geheizt oder gekühlt ist, wird untersucht, um den Einfluß der Auftriebskräfte auf die ursprüngliche erzwungene Konvektionsströmung zu bestimmen. Alle möglichen Anstellwinkel einschließlich der Sonderfälle horizontale und vertikale Platte können durch die Berücksichtigung beider Komponenten der Vektors der Erdbeschleunigung, normal und parallel zur Oberfläche, erfasst werden. Die Untersuchung wird vervollständigt durch eine Variation der thermischen Randbedingung und der Prandtl-Zahl (wird in Teil II abgehandelt). Ein bemerkenswertes Ergebnis dieser Arbeit ist die Erkenntnis, daß bei auftriebsinduzierter Ablösung sowohl singuläres als auch reguläres Verhalten am Ablösepunkt auftreten kann.

СМЕШАННАЯ КОНВЕКЦИЯ ОТ ПОЛУБЕСКОНЕЧНОЙ ПЛОСКОЙ ПЛАСТИНЫ С ПРОИЗВОЛЬНЫМ УГЛОМ НАКЛОНА—I. ЭФФЕКТ УГЛА НАКЛОНА

Аннотация—С целью определения влияния подъемных сил на вынужденную конвекцию исследуется ламинарный пограничный слой на полубесконечной плоской пластине с произвольным углом наклона, которая нагревается или охлаждается. Анализируется широкий диапазон углов наклона (включая особые случаи горизонтальной и вертикальной пластин) при учете обеих компонент вектора силы тяжести, т.е. поперечной и продольной относительно поверхности. Варьирование свободных параметров осуществляется за счет использования различных тепловых граничных условий и изменения числа Прандтля (см. вторую часть работы). Одним из наиболее существенных результатов работы является установление того факта, что при действии противоположно направленных сил может наблюдаться как сингулярное, так и регулярное поведение.